HM and THM interactions in bentonite engineered barriers for nuclear waste disposal

Antonio Gens[1]*, Jordi Alcoverro[1], Radim Blaheta[2], Martin Hasal[3], Zdeněk Michalec[2], Yusuke Takayama[4], Changsoo Lee[5], Jaewon Lee[5], Geon Young Kim[5], Chia-Wei Kuo[6], Wan-Jung Kuo[6], Chung-Yi Lin[6]

[1] UPC - CIMNE

[2] The Czech Academy of Sciences, Institute of Geonics (IGN)

[3] The Czech Academy of Sciences, Institute of Geonics (IGN) - IT4Innovations, VŠB, Technical University of Ostrava, Ostrava, Czech Republic

[4] Japan Atomic Energy Agency (JAEA)

[5] Korea Atomic Energy Research Institute (KAERI)

[6] CAMRDA, National Central University, Taiwan (NCU)

* Corresponding author: Antonio Gens, e-mail: antonio.gens@upc.edu, telephone: +34-639519055

- stReports the work performed in a DECOVALEX 2019 Task (INBEB) aimed to study the hydro-mechanical and thermo-hydro-mechanical interactions in bentonite engineered barriers using numerical analyses.
- Bentonite engineered barriers are a key component of many designs of deep geological repositories for high level nuclear waste and spent fuel
- TH and THM coupled numerical analyses of two large scale tests (EB and FEBEX) are performed by four modelling teams
- Simulation results are compared with field observations corresponding to measurements obtained during the performance of the tests and during dismantling operations
- The performance of the various modelling approaches in relation to the observed TH and THM barrier behavior is evaluated and discussed

Abstract

Bentonite-based engineered barriers are a key component of many repository designs for the confinement of high-level radioactive waste and spent fuel. Given the complexity and interaction of the phenomena affecting the barrier, coupled hydro-mechanical (HM) and thermo-hydro-mechanical (THM) numerical analyses are a potentially useful tool for a better understanding of their behaviour. In this context, a Task (INBEB) was undertaken to study, using numerical analyses, the hydro-mechanical and thermo-hydro-mechanical Interactions in Bentonite Engineered Barriers within the international cooperative project DECOVALEX 2019. Two large scale tests, largely complementary, were selected for modelling: EB and FEBEX. The EB experiment was carried out under isothermal conditions and artificial hydration and it was dismantled after 10.7 years. The FEBEX test was a temperature-controlled non-isothermal test combined with natural hydration that underwent two dismantling operations, a partial one after 5 years of heating and a final one after a total of 18.4 years of heating. Direct observation of the state of the barriers was possible during the dismantling operations so that the evolution of barrier heterogeneity under transient conditions could be determined. Four teams performed the HM and THM numerical analyses using a variety of computer codes, formulations and constitutive laws. For each experiment, the basic features of the analyses are described and the comparison between calculations and field observations are presented and discussed. Comparisons involve measurements performed during the performance of the test and data gathered during dismantling. A final evaluation of the performance of the modelling closes the paper.

Keywords

DECOVALEX, engineered barriers, bentonite, THM formulations, coupled numerical analyses, large-scale tests

1. Introduction

Deep geological repository systems for high-level radioactive waste and spent fuel are generally based on a multi-barrier approach in which a series of barriers (e.g. canister, bentonite barrier, host rock) jointly contribute to an appropriate long-term confinement of the waste. In this context, bentonite-based engineered barriers are often a key component of the deep geological repository designs for nuclear waste. In the most general case, the barrier is subject to complex interacting phenomena comprising the heat released by the waste, the intake of water from the host rock and the subsequent development of swelling pressure as hydration progresses[1]. Figure 1 shows, in a schematic way, some of the thermo-hydro-mechanical (THM) processes involved in the evolution of the barrier during this transient saturation period. The radioactive waste emits heat that is transported through the bentonite to the rock producing a temperature rise that reduces as the distance to the waste increases. The temperature rise produces water evaporation in the inner part of the barrier that results in a drying the bentonite. Vapour migrates towards the outer regions of the barrier where it condenses due to the lower temperature prevailing there. Because the bentonite is unsaturated and, therefore, under suction, water flows from the host rock to the barrier. Consequently, the barrier hydrates, starting in the outer zones close to the rock and progressively moving inwards. Because of the low permeability of bentonite and host rock, hydration proceeds quite slowly but it is expected that the barrier will become fully saturated in the long term. Associated with those thermo-hydraulic phenomena there also mechanical effects: bentonite deformation due to changes in temperature, suction and stresses and development of the bentonite swelling stress as hydration progresses. In some applications such as bentonite seals, away from the waste, the thermal component is minor and only hydro-mechanical (HM) processes are relevant. In any case, a proper understanding of the processes occurring during the transient period, requires the appropriate simulation of the evolution of the engineered barrier by means of coupled numerical analyses.

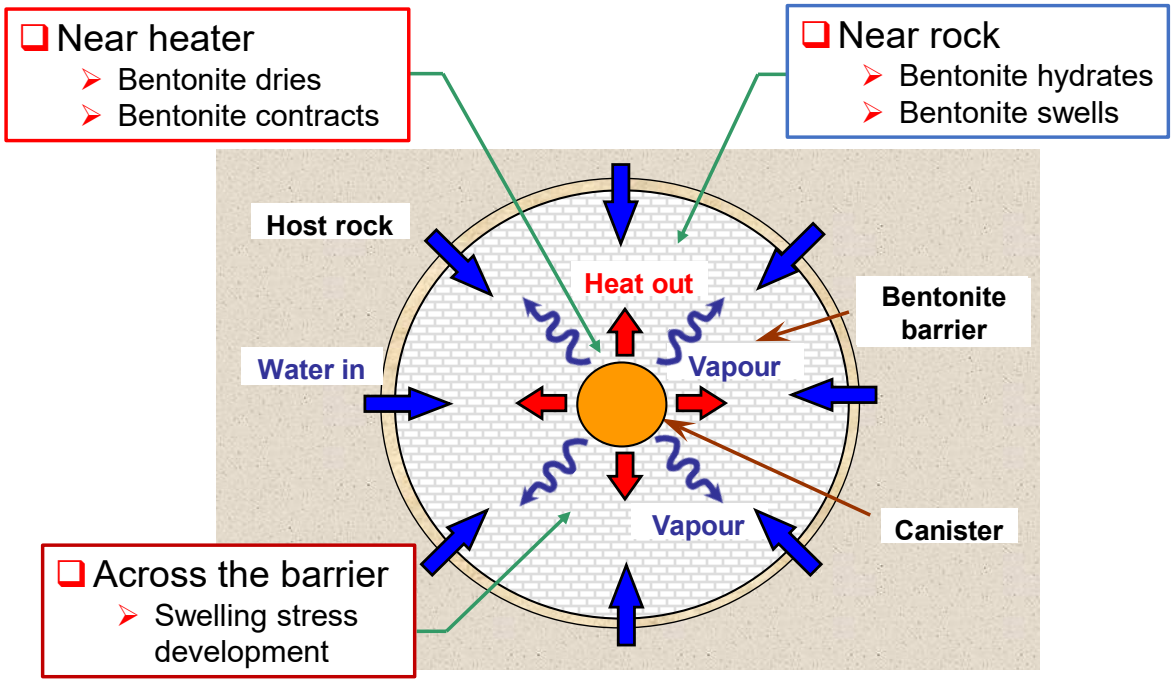

Figure 1. THM processes involved in the evolution of the barrier during the transient period

The complexity of the ensemble of coupled processes involved leads to considerable uncertainty about the state of the barrier at the end of the transient period. In this respect, a Task, within the international cooperative project DECOVALEX 2019[1], was undertaken to study the hydro-mechanical (HM) and thermo-hydro-mechanical (THM) INteractions in Bentonite Engineered Barriers (INBEB). Special attention was paid to the evolution of barrier heterogeneity under transient conditions and to the final state of the barrier. As dry density is directly related to a number of safety functions of the bentonite barrier, its distribution at the end of the transient period is clearly relevant.

Very timely, two long-term large-scale tests (EB and FEBEX) in which the final state of the barrier had been directly observed after dismantling had become available to the Task. The two experiments provided unambiguous information on the condition of the bentonite barrier after a long transient period developed under realistic field conditions. The experiments encompass a range of barrier configurations and test settings and are, in many respects, complementary. The EB (Engineered Barrier) experiment was carried

[1] DECOVALEX is an acronym for DEvelopment of COupled models and their VALidation against EXperiments

out in the Mont Terri underground laboratory; the barrier was made up of granular bentonite with the addition of some bentonite blocks providing support for a dummy canister. The test was carried out under isothermal conditions and artificial hydration. Dismantling took place after 10.7 years of testing. The FEBEX (Full-scale Engineered Barrier EXperiment) test was performed at the Grimsel Test Site; the barrier is composed of bentonite blocks only. It is a temperature-controlled non-isothermal test combined with natural hydration from the rock. The FEBEX experiment underwent two dismantling operations, a partial one after 5 years of heating and a final one after a total of 18.4 years of heating, thus allowing the direct determination of the state of the engineered barrier at two different times.

The INBEB Task involved the performance of numerical analyses of the EB and FEBEX experiments by a number of modelling teams. The results obtained were compared with observations gathered both during the performance of the tests and from their dismantling. It was not a blind prediction exercise as the results of the experiments were published and available to the modellers. The numerical analyses were undertaken by four teams: Institute of Geonics, of the Czech Academy of Sciences (IGN), supported by SÚRAO, Czech Republic, Japan Atomic Energy Agency (JAEA), Korea Atomic Energy Research Institute (KAERI) and National Central University of Taiwan (NCU), supported by Taipower.

The paper presents a summary account of the wok carried out within the INBEB Task and assesses the capabilities of numerical formulations and codes to simulate and interpret the observed HM and THM behaviour of the bentonite barriers, with a particular focus on the final state reached upon saturation. It is structured as follows: for each of the two tests, the experiment is briefly described first, the main features of the analyses are then reported and selected comparisons between numerical results and field observations are presented and discussed. An overview and concluding remarks section closes the paper. Additional information on the work is available in the final INBEB Task report[2].

2. EB test: description

The Engineered Barrier Emplacement (EB) Experiment was performed in the Mont Terri underground rock laboratory located near Saint-Ursanne in northern Switzerland and excavated in Opalius clay, a stiff strongly layered shale[3]. The experiment involved the artificial hydration of an engineered barrier made up of granular bentonite and compacted bentonite blocks[4]. It was carried out in the EB niche, a 15 m long drift with a horseshoe section (2.25 m high, 3.00 m wide) excavated for the purpose. In the last 6 m of the drift, a dummy canister was placed horizontally over a bed of compacted bentonite blocks; the remaining space was filled with a granular bentonite material made of highly compacted bentonite pellets. The dummy canister was a carbon steel cylinder (4.54 m long, 0.97 m in diameter) with a weight of 110 kN. A concrete plug isolated the test setup. A longitudinal section and a cross-section of the experiment are shown in Figures 2 and 3, respectively. Figure 4 shows the dummy canister sitting on a bed of compacted bentonite blocks.

Three layers of bentonite blocks were used to provide a bed for the dummy canister. They had a dry density of 1.69 g/cm^3 and a mass water content of 14.4%. The granular bentonite was placed by gravity fall from an auger that accessed the test section through an opening in the retaining wall. The backfill proceeded from the end of the drift towards the front of the test section (Figure 5). The total mass of granular bentonite emplaced in the test was 40.2 tons filling an estimated volume of about 28.4 m^3. The mass water content of the pellets was 4.2 %. From the emplacement data, an average dry density of 1.36 g/cm^3 was calculated for the granular bentonite. It was not possible to determine whether there were significant heterogeneities in the initial dry density distribution; it is however quite possible that some segregation may have occurred during installation.

The experiment was instrumented with 54 sensors that measured the evolutions of relative humidity (RH), pore pressure, total pressure and displacement. They were placed in seven instrumented sections of the bentonite barrier and in a number of boreholes located in the rock. Only the measurements of the sensors installed in the bentonite are considered in this paper.

FEBEX bentonite was used for both the compacted blocks and the granular material constituting the engineered barrier. The material has been obtained from a quarry in the volcanic zone of Serrata de Níjar in South-Eastern Spain. It has a high smectite content, in the range of 88%–96%, with small and variable quantities of accessory minerals such as quartz, calcite and feldspars. The cation exchange capacity is 100–102 meq/100 g (42% Ca, 33% Mg, 23% Na, 2% K). The range of the liquid limit is 98%-106% and of the plastic limit 50%-56%. The FEBEX bentonite, in block and granular form, has been the object of intense characterization in the laboratory[5-11]. A synthesis of the available information on the THM properties of the bentonite was made available to the modelling teams.

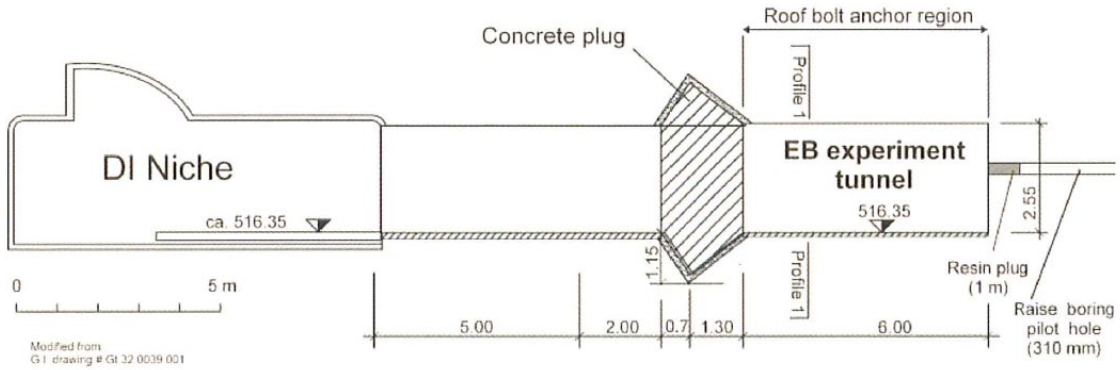

Figure 2. Longitudinal section of the EB experiment and niche

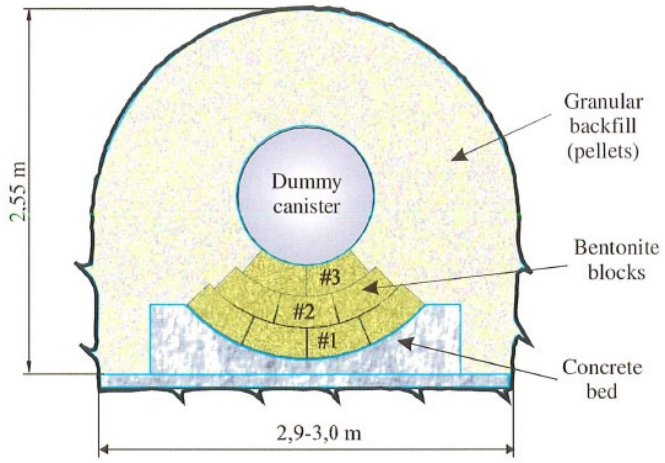

Figure 3. Cross- section of the EB experiment

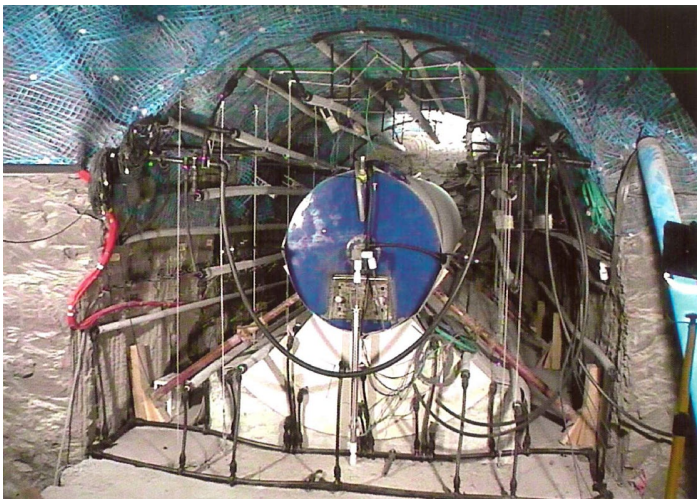

Figure 4. Dummy canister sitting on a bed of compacted bentonite blocks. The pipes for the artificial hydration system can be noted.

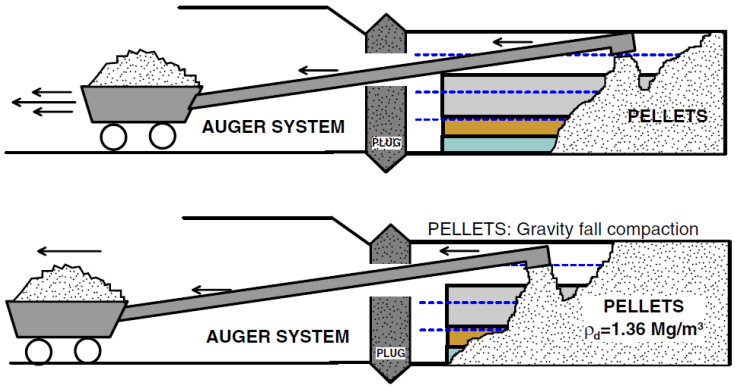

Figure 5. Scheme for the emplacement of granular bentonite

Due to the low permeability of the Opalinus Clay formation, artificial hydration was adopted to ensure a faster saturation. The hydration system comprised a network of distribution pipes with injectors and geotextile hydration mats placed between bentonite blocks and around the canister (Figure 4). During the first 5.1 years of operation (May 2002 to June 2007), water was directly injected into the barrier; a water with a chemical composition similar to that of the water in the Opalinus Clay formation was used. Figure 6 shows the evolution of the volume of water injected. It should be noted that the amount of water is well above the pore volume available in the test, indicating some water loss. Leaks were in fact observed, especially in the initial hydration period and the amount of water potentially lost through the Opalinus Clay

formation and the concrete plug could not be quantified. During the subsequent 5.6 years (July 2007 to January 2013), only natural hydration from the Opalinus Clay formation took place.

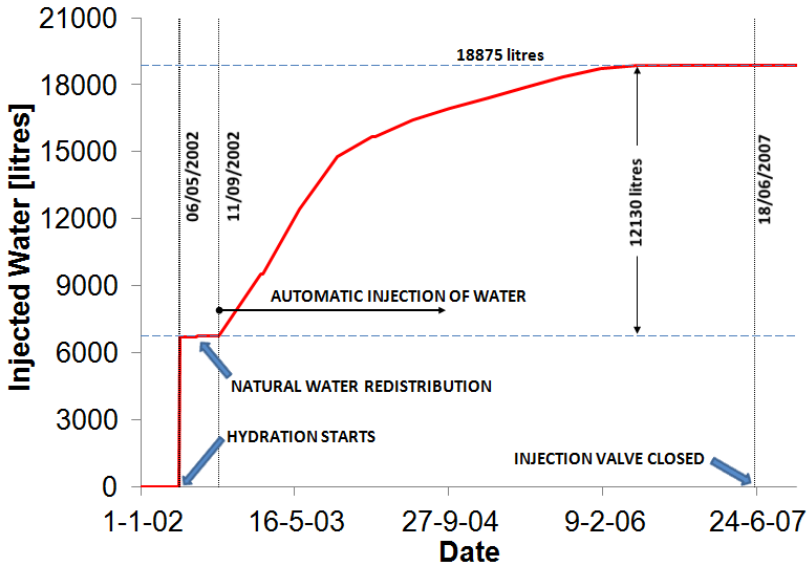

Figure 6. Evolution of the injected water volume with time

After 10.7 years of operation, the experiment was dismantled and the state of the barrier examined[12]. In order to characterize the final state of the EB experiment, both the clay barrier and other test elements were visually inspected and were subjected to intensive sampling for laboratory testing, mainly focused on the bentonite buffer. Dry densities and mass water contents were determined on-site immediately after recovering the samples from the barrier. A field laboratory was established for this purpose. It was found that the barrier had become largely saturated at the time of dismantling.

A series of results were requested from the modelling teams concerning the evolution of displacements of the canister, the evolution of the relative humidity in the granular bentonite and in the bentonite blocks, and the evolution of total pressures. In addition, distributions of dry density, water content and degree of saturation at the end of the experiment were also required.

It should be noted, however, that the EB experiment had some limitations that hinder, to some degree, the interpretation of the observations and the detailed assessment of the modelling. They are:

- The EB test was mainly a demonstration experiment, so the amount of instrumentation installed was limited.
- There was leakage of water towards the outside of the experiment that could not be quantified. The measured water intake exceeds significantly the pore volume available for water filling.
- The hydration history is very complex. Moreover, only the global water intake and overall pressure were monitored. It was not possible, therefore, to identify the history of water inflow for each individual injection point. In addition, the actual water intake was uncertain because of leaks.
- The fact that horizontal canister movements were measured indicates that hydration was not symmetrical although the test layout was.
- The initial degree of homogeneity of dry density throughout the granular backfill is unknown. It is likely that some material segregation took place during the emplacement of the pellets. A degree of heterogeneity in the backfill at the start of the test is therefore quite likely.

3. EB test: modelling features

The main features of the analysis for the different modelling teams are collected in Table 1; it can be noted that a variety of computer codes have been used. All teams employed a coupled hydro-mechanical formulation involving the solution of the corresponding hydraulic (water mass balance and liquid flow) and mechanical (equilibrium) equations. KAERI also incorporated and solved the air balance and gas flow equations. In the case of NCU the coupling operated from the hydraulic to the mechanical problem but not in the opposite direction.

There is a common core in the hydraulic formulations and associated constitutive laws. Water flow is governed by Darcy's law with hydraulic conductivity dependent on degree of saturation via a relative

permeability relationship, commonly represented by a power law. IGN and KAERI also incorporate the variation of intrinsic permeability with dry density. Retention curves are generally defined by expressions based on the van Genuchten functions[13]. Vapour flow was included in the IGN and KAERI formulations although its effect is not significant in this isothermal case. The main departure from the standard conventional hydraulic formulation has been introduced by IGN by considering the presence of the water in the pores and in the interlayer space. Degrees of saturation higher than 100% can then be computed because the total amount of water is referred to the volume of the bulk pores only, i.e. excluding the interlayer volume that also contains water[14]. In fact, degrees of saturation of more than 100% have been measured in highly compacted FEBEX bentonite, usually attributed to a higher density of the water in the interlayer space[5,15]. Most mechanical constitutive models are based on elasticity with the addition of a specific swelling term. KAERI uses instead an elasto-plastic model, BBM[16], in which unsaturation effects are accounted for by the dependency of the yield surface on suction.

Table 1. Main features of the EB analyses

Team	Coupling	Computer code	Geometry	Variable intrinsic permeability	Vapour transport	Mechanical constitutive model
IGN	H < > M	COMSOL 3D	3D	Yes	Yes	Non-linear elastic + swelling term
JAEA	H < > M	THAMES 3D	3D (one slice)	No	No	Non-linear elastic + swelling term
KAERI	H < > M	TOUGH2-MP (H) + FLAC 3D (M)	2D plane strain	Yes	Yes	Elasto plastic model (BBM)
NCU	H > M	HYDROGEOCHEM 4.3	2D plane strain	No	No	Linear elastic + swelling term

All the modelling teams simulated the full sequence of the experiment including excavation and ventilation of the tunnel, artificial hydration stage, natural hydration and dismantling. Only JAEA did not consider the initial ventilation phase. IGN used a 3D domain for the analyses whereas the other teams opted for a 2D plane strain configuration (the 3D slice of JAEA is effectively a 2D plane strain geometry). The initial conditions of the analyses in terms of porosity, water content, degree of saturation and relative humidity are presented in Table 2. All teams adopt similar values except IGN that considered a non-uniform

dry density distribution in the pellets to account for possible segregation during emplacement. Parameters were determined based on the information supplied in the case specifications, references in technical literature and their own modelling expertise. Table 3 lists the main hydraulic and mechanical parameters selected by the different teams. IGN adopted alternative values of permeability for the first two days of intense hydration to take into account the open structure of the pellets, using a larger value for the flow in the downward and horizontal direction than for the upward direction. There is more variation among the teams regarding swelling pressure, reflecting the larger variation associated with the mechanical constitutive laws. The swelling pressure of pellets is notably lower than that of the blocks reflecting their porosity difference.

Table 2. Initial conditions

Team	Initial dry density (g/cm^3)	Initial porosity	Initial mass water content (%)	Initial degree of saturation (%)	Initial suction (MPa)	Initial relative humidity (%)
	Blocks					
IGN	1.69	0.37	14.4	55.3	120	40.0
JAEA	1.69	0.37	14.0	63.0	123	40.0
KAERI	1.69	0.37	11.15	50.4	125	40.0
NCU	1.69	0.37	14.7	66.2	125	40.7
	Granular bentonite (pellets)					
IGN	1.26 - 1.46	0.46 - 0.53	3.5	7.0-8.9	400	5.2
JAEA	1.36	0.50	4.0	12.0	1000	4.0
KAERI	1.36	0.50	6.9	19.0	450	3.5
NCU	1.36	0.50	6.8	18.7	450	3.9

Table 3. Main initial hydraulic and mechanical parameters

	Initial unsaturated permeability Blocks (m^2)	Initial saturated permeability Blocks (m^2)	Initial unsaturated permeability Pellets (m^2)	Initial saturated permeability Pellets (m^2)	Rock saturated permeability (m^2)	Initial swelling pressure* Block/Pellets (MPa)
IGN	$4.50\ 10^{-22}$	$2.67\ 10^{-21}$	(1)	(1)	$5.00\ 10^{-20}$	7.5/0.47-1.7
JAEA	$3.70\ 10^{-22}$	$3.10\ 10^{-21}$	$2.50\ 10^{-22}$	$2.10\ 10^{-19}$	$2.30\ 10^{-20}$	10/0.48
KAERI	$2.08\ 10^{-22}$	$5.00\ 10^{-21}$	$1.19\ 10^{-21}$	$2.00\ 10^{-18}$	$5.00\ 10^{-20}$	2.63/0.35
NCU	$6.48\ 10^{-22}$	$2.39\ 10^{-21}$	$6.21\ 10^{-21}$	$1.63\ 10^{-19}$	$1.78\ 10^{-20}$	6.62/0.09

(*) Swelling pressure under 1-D oedometric conditions

(1) The first two days of intensive hydration, intrinsic permeability is 10^{-16} m^2 in the horizontal and downward direction and 10^{-18} m^2 in the upward direction. Afterwards, standard permeability values are adopted.

4 EB test: modelling results

In this section, numerical model results are compared with field observations. The codes and labels used for the modelling teams and for the experimental observations are shown in Table 4. Only some results are reported herein, selected to illustrate the main outcomes of the analyses.

Table 4. Codes and symbols assigned to the modelling teams and observations

Modelling team	Code	Symbol
Institute of Geonics of the Czech Academy of Sciences (IGN)	IGN	■
Japan Atomic Energy Agency (JAEA)	JAE	◆
Korea Atomic Energy Research Institute (KAERI)	KAE	◇
National Central University of Taiwan (NCU)	NCU	▲
Experiment observations	CIM	●

As expected, all the RH sensors in the granular bentonite indicated a progressive hydration leading to saturation (RH=100%). However, it was observed that there were large differences in the time-evolution of RH of the various sensors, which did not seem to follow a logical pattern; they were probably affected by local measurement and flow conditions. Saturation times for different sensors varied between 170 days and more than 500 days. This lack of pattern makes it difficult to evaluate the modelling results. As an example, the computed and observed evolutions of RH of one sensor installed in the granular bentonite are plotted in Figure 7. A range of computed hydration rates were obtained from the different analyses that can be traced back to differences in the initial and subsequent values of permeability. The time-evolution of the RH measured in sensors located in the bentonite blocks appear to be generally more consistent, showing saturation times within a narrower range (200-280 days). In this case, all modelling results seem to provide a reasonable reproduction of the test data, given the uncertainty of the measurements (Figure 8).

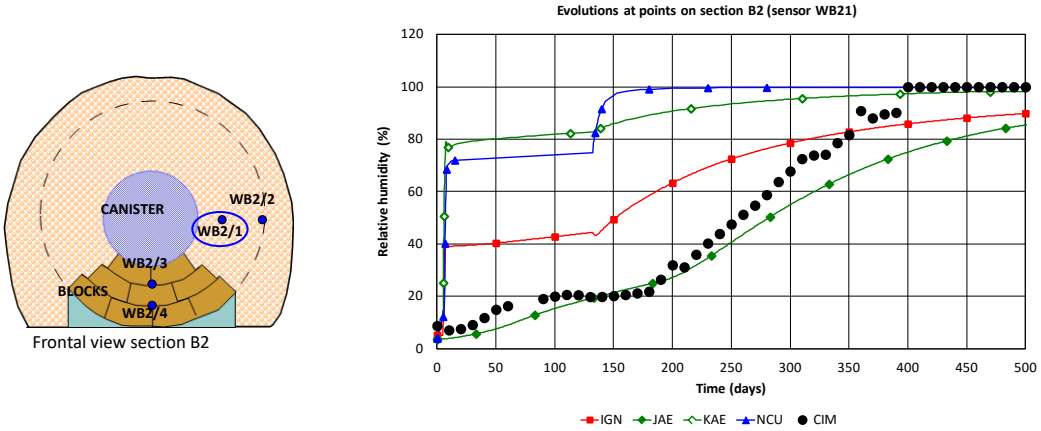

Figure 7. Modelling results vs. observations. Relative humidity in the granular bentonite. Sensor W2/1, Section B2

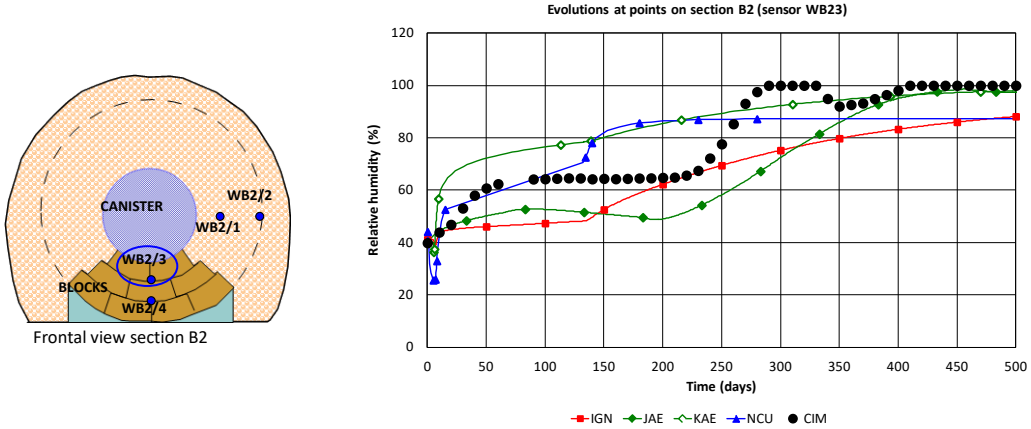

Figure 8. Modelling results vs. observations. Relative humidity in the bentonite blocks. Sensor W2/3, Section B2

The comparisons between modelling results and measurements of total stress are shown in Figure 9 and 10 for two typical sensors emplaced on the interface barrier/rock; the sensor of Figure 9 measures vertical stress and the sensor of Figure 10 measures horizontal stress. The stress measurements showed a progressive development of swelling pressures, the final values were reached at times above 1500 days, much longer than those corresponding to achieving 100% RH. The final stresses measured lie in the range of 1.5 MPa to 2.3 MPa. It is also noted that the observed values of total stresses are somewhat lower in the horizontal direction, but differences are small and the degree of stress anisotropy is therefore not very significant. Most swelling stress evolutions reported by the modelling teams exhibit a progressive increase

with time reaching, consistent with observations, the final values at quite long times, suggesting that the mechanical constitutive laws generate particularly strong swelling when close to saturation. IGN and KAERI report vertical stresses in the observed range of values, smaller stresses are computed by JAEA and NCU. KAERI reports values of total stresses in the horizontal direction quite close to the observed ones. In contrast, the three other teams report significantly lower values compared to the vertical ones. The reason is unclear as the mechanical constitutive models are all isotropic.

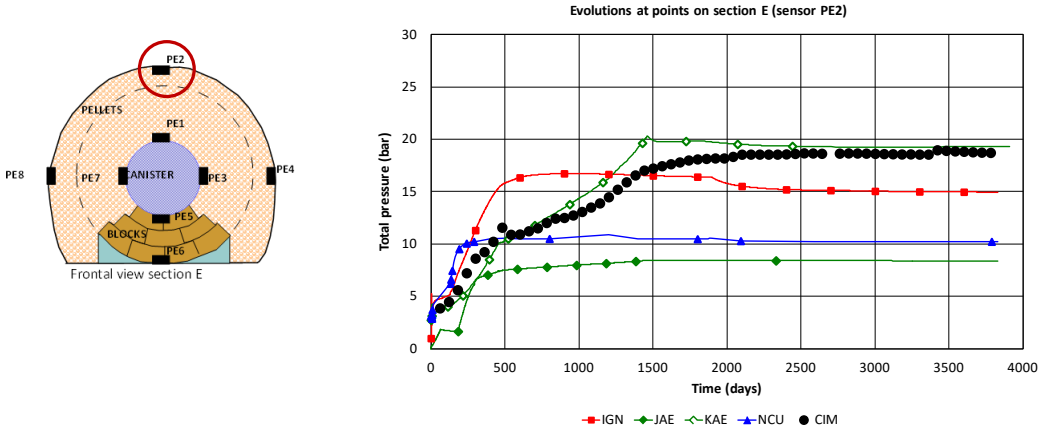

Figure 9. Modelling results vs. observations. Total vertical stress. Section E, sensors PE2.

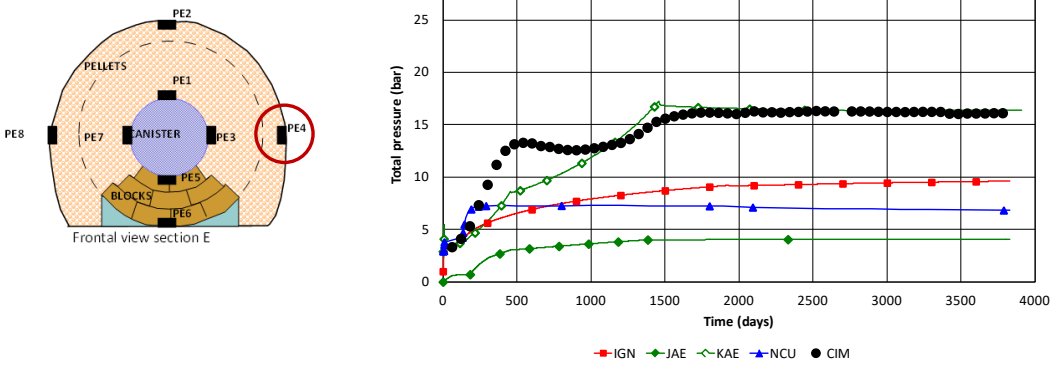

Figure 10. Modelling results vs. observations. Total horizontal stress. Section E, sensors PE4.

During dismantling, numerous samples were extracted, their dry density and water content were determined immediately after extraction. It was found that the bentonite barrier had become largely saturated throughout. With few exceptions, measured degrees of saturation were 95% and higher. A few values above 100% were measured (with a maximum of 105%) not showing any clear spatial pattern. The

most remarkable observation was a very high degree of homogenization in the vertical direction between blocks and granular bentonite in all the sampled sections. Dry density values in the range of 1.35 g/cm^3 - 1.40 g/cm^3 were measured irrespective of whether the location of the sample corresponded to the granular bentonite or to a block. For reference, the initial dry density was 1.69 g/cm^3 for the blocks and 1.36 g/cm^3 for the granular bentonite. Figure 11 shows contours of measured dry density in three different sections; vertical homogenization is readily apparent. Another significant feature of the observations is the low dry density in the zones close to the lower corners of the cross-sections (measurements often in the range 1.1 g/cm^3 - 1.2 g/cm^3). In the rest of the section, rather uniform dry density conditions prevail with practically all values in the range 1.3 g/cm^3 - 1.4 g/cm^3 without a clear pattern of variation within this range. As the barrier was practically saturated everywhere, the measured mass water contents were directly related to dry density.

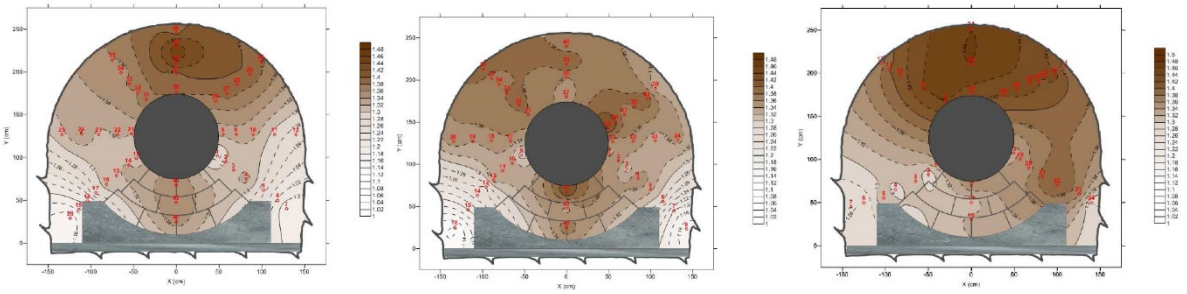

a) b) c)

Figure 11. Contours of dry density measured on dismantling. a) section A1-25, b) section E, c) section C

Typical comparisons between the computed and measured degree of saturation are presented in Figures 12 and 13 for two vertical radii; Figure 12 corresponds to the pellets zone and Figure 13 to the blocks zone. Degree of saturation is not a direct measurement as water content is; densities are also required for its calculation. However, comparisons are established in terms of degree of saturation rather than water content because it provides definite information on how close a particular point (or the barrier as a whole) is to saturation. If water content is used, it is always necessary to refer to the corresponding dry density to have a measure on how much hydration has progressed.

IGN, KAERI and NCU report high degrees of saturation for the final state of the barrier, generally above 90%; consistent with observations. IGN reports degrees of saturation well above 100% (up to more

than 110%) largely in the zone occupied by blocks; a consequence of considering interlayer water in their formulation. It should be noted, however, that, in contrast with the modelling results, the few points where degrees of saturation higher than 100% were measured do not correspond to the zone occupied by blocks. In contrast, JAEA computes degrees of saturation at the end of the analysis of the order of 75% in the pellets zone, quite far from saturation in spite of the fact that the computed rate of hydration (in terms of relative humidity) appears reasonable consistent with observations. The reported final low degree of saturation is likely due to the use of an initial pellets permeability lower than those of the other teams. This slower hydration may also account for the fact that the swelling stresses computed by JAEA are generally low compared to other teams and observations.

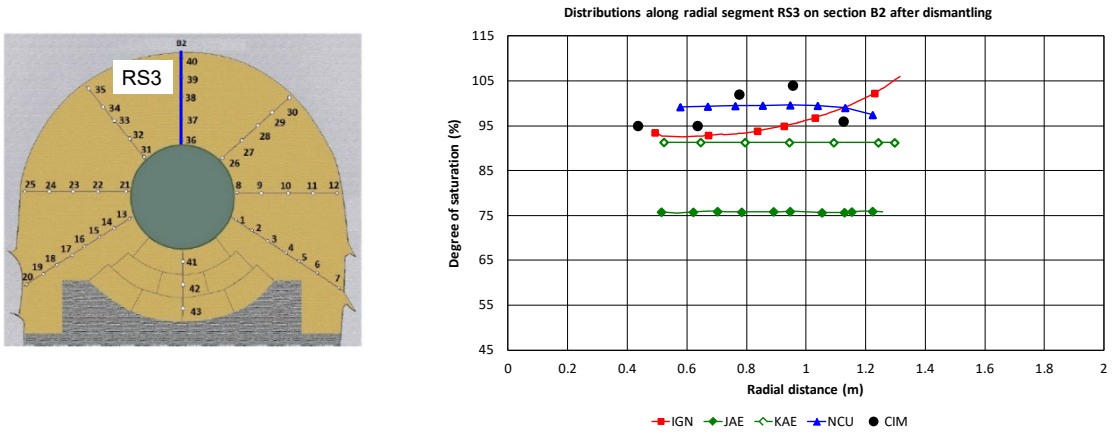

Figure 12. Distributions of degree of saturation. Modelling results vs. observaitons. Section B2, segment RS3 (pellets)

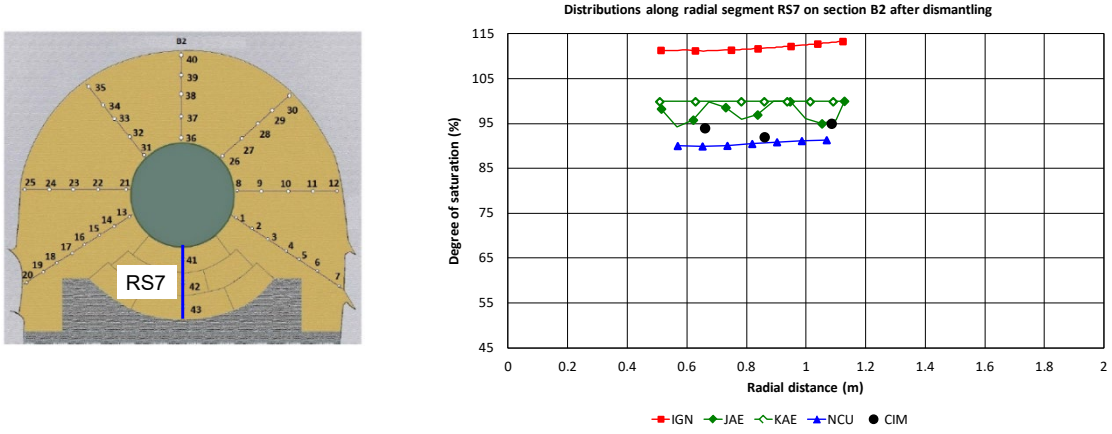

Figure 13. Distributions of degree of saturation. Modelling results vs. observaitons. Section B2, segment RS7 (blocks)

Representative comparisons concerning the distributions of dry density are presented in Figures 14 to 17. The vertical homogenization of the barrier can be noted by referring to Figures 14 and 15. In the pellets section (Figure 14), there has been a modest increase of dry density whereas in the blocks the reduction in dry density is very large (Figure 15). As a consequence, the dry density is practically the same in the two zones.

The degree of homogenization blocks-granular bentonite in the vertical direction is underestimated by IGN, JAEA and KAERI. The results showing the largest homogenization are those provided by IGN although they are still not close to observations. Because the current state of the NCU formulation does not allow to compute the changes in porosity due to suction and stress changes, the dry density distributions reported are constant and equal to the initial values.

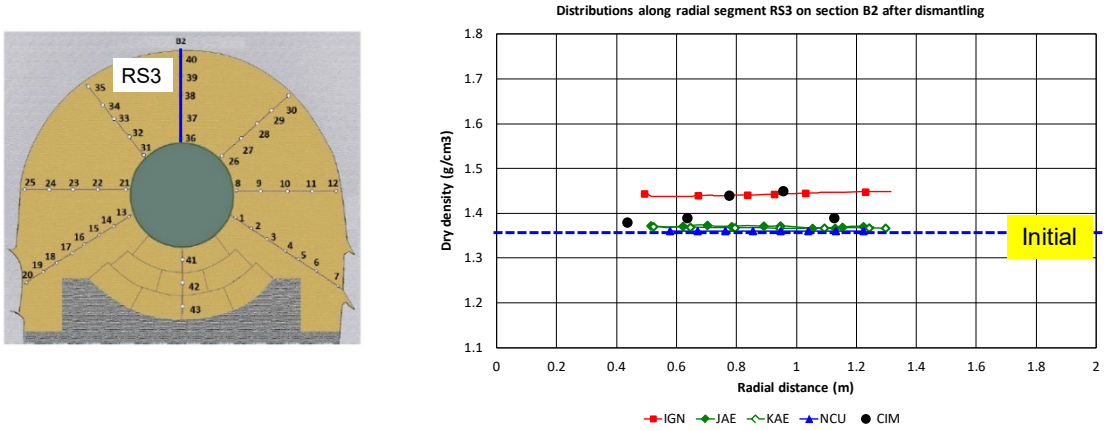

Figure 14. Distributions of dry density. Modelling results vs. observations. Segment RS3, Section B2. The initial average dry density value of the pellest is indicated.

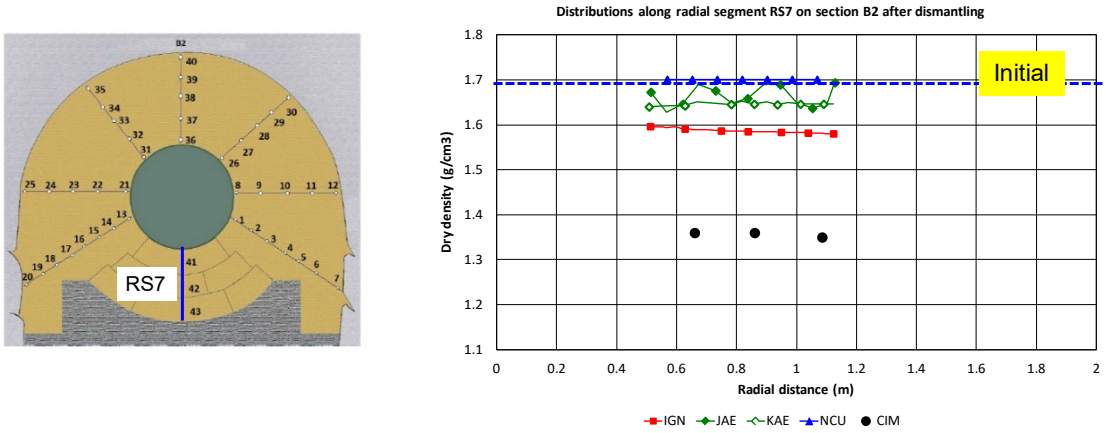

Figure 15. Distributions of dry density. Modelling results vs. observations. Segment RS7, Section B2. The initial dry density value of the blocks is indicated.

Figure 16 shows the comparison of dry density distributions for a segment in the low dry density area at the lower corners of the section. It can be noted that this zone of low dry density is not reproduced by any of the modelling teams. It is likely, however, that such low dry density is related to the heterogeneity of the initial placement of the granular bentonite and, therefore, it should not be expected to be an outcome of models where initial homogenous conditions are assumed. The assumption by IGN of a linear variation of dry density with depth leads to lower dry density values at those locations but they are still far from the observations. A good reproduction of dry densities is achieved in the rest of the barrier where the change of dry density from initial conditions has been small (e.g. Figure 17).

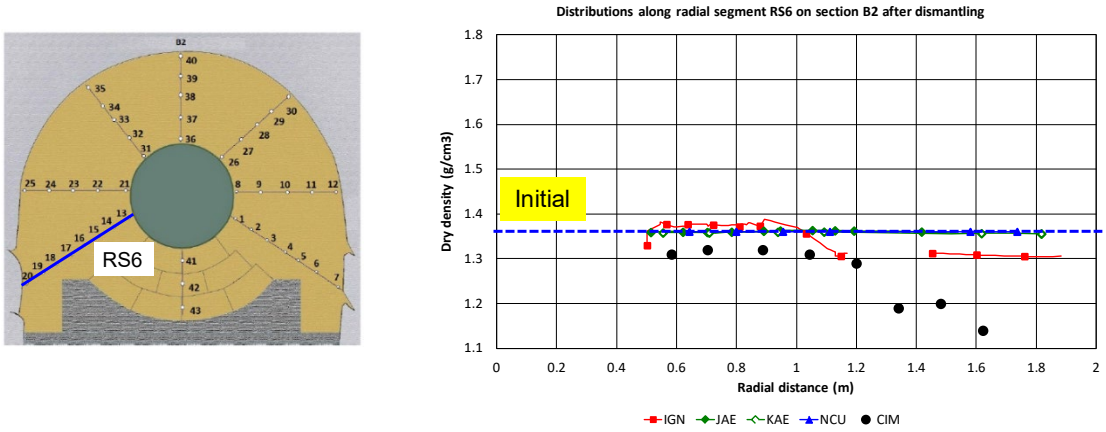

Figure 16. Distributions of dry density. Modelling results vs. observations. Segment RS6, Section B2. The initial average dry density value of the pellets is indicated.

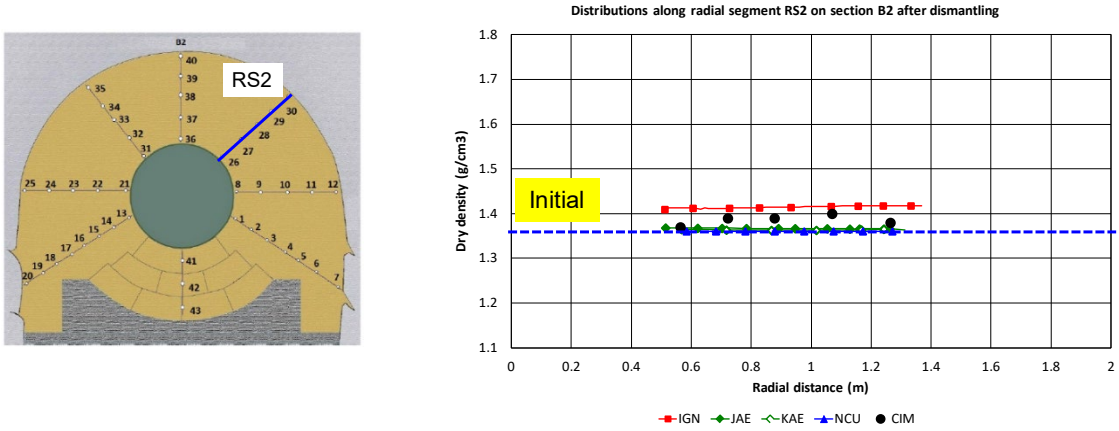

Figure 17. Distributions of dry density. Modelling results vs. observations. Segment RS2, Section B2. The initial average dry density value of the pellets is indicated.

5. EB test: discussion

As indicated in section 2, there are a number of significant shortcomings in the EB experiment that thwart the interpretation of the observations and prevent a more discriminating assessment of the modelling performed. In any case, all the modelling teams reproduced the general hydromechanical behaviour observed during the operation of the test, i.e. a progressive increase of relative humidity and an associated development of swelling pressures. The final quasi-saturated state of the barrier was generally well reproduced by IGN, KAERI and NCU. Saturation at the end of the test was not predicted by JAEA probably because of the use of a lower initial permeability for the pellets.

The final total stresses developed in the test were adequately reproduced by IGN and KAERI whereas JAEA and NCU report smaller values for the sensors located in the pellets. Only KAERI, however, obtains a nearly isotropic state of stresses with similar values in the horizontal and vertical directions, consistent with observations. Considering the results of the EB test globally (hydration, development of swelling pressures, final saturation of the barrier), KAERI arguably produced the more representative modelling overall.

However, regarding one of the main objectives to the Task: the prediction of the final degree of homogenization of the barrier, the results were not fully satisfactory. Leaving aside the low barrier dry density at the lower corners of the cross section (probably a consequence of initial emplacement

heterogeneity), the significant feature of a nearly complete homogenization between blocks and granular bentonite in the vertical direction was not captured by any modelling team. It is possible that more advanced constitutive models for the mechanical behaviour of blocks and pellets may be required to achieve this result.

In any event, it is not precisely known what the basic cause for this nearly full homogenization is and how it depends on the rate, sequence and other details of the process of hydration. This uncertainty is related to a basic limitation of one-off large-scale tests where it is often difficult to pinpoint unambiguously to the specific effects of the different phenomena that impact the observed global behaviour of the experiment. The lack of reliable information about the initial state of the barrier is also a significant contributor to this uncertainty.

6. FEBEX test: description

The FEBEX test is a heating experiment, carried out in the Grimsel Test Site (GTS) intended as a full-scale demonstration of the Spanish reference concept for a high-level waste disposal system. The GTS is excavated in the granite rocks of the Aare Massif of Central Switzerland[17]. The test was installed in a 70.4 m long, 2.28 m diameter circular tunnel especially excavated for the purpose using a Tunnel Boring Machine (TBM). The experiment area occupied a section 17.4 m-long at the far end of the tunnel. The general layout consisted of two heaters (each 4.54 long, 0.9 m diameter and 110 kN weight) surrounded by an engineered barrier made up of compacted FEBEX bentonite blocks (Figures 18 and 19). A total of 5331 bentonite blocks were installed manually with an average mass water content of 14.4% and an average dry density of 1.69 g/cm^3. Because of technological voids and joints between the blocks, the average dry density of the bentonite, considering the full tunnel volume, was 1.60 g/cm^3. A 15 mm-thick perforated steel liner was emplaced between the heaters and the bentonite blocks and a 2.40 m long concrete plug isolated the test area. A total of 632 sensors were installed in the bentonite barrier, the surrounding rock and in the test adjacent areas; only sensors located in the bentonite are considered here (Figure 18). The main variables

measured in the barrier were temperature, relative humidity and total normal stresses. The power applied to the two heaters was also recorded.

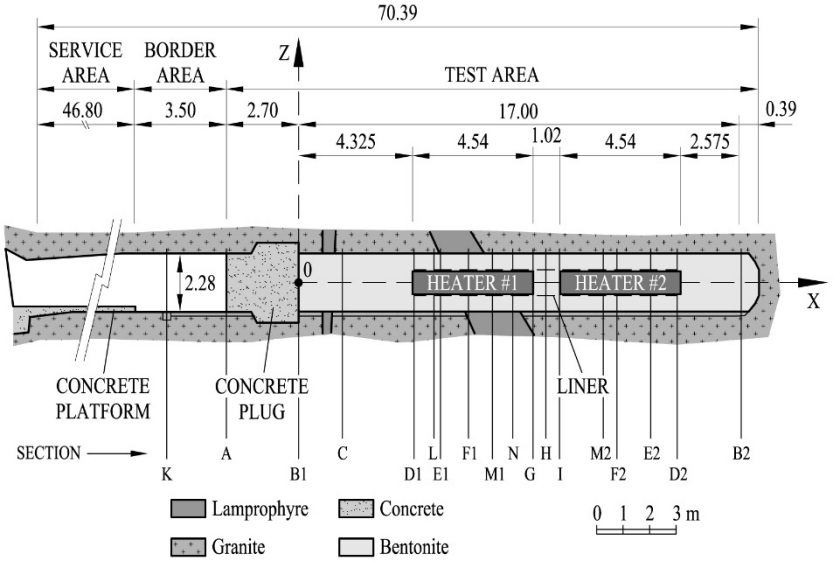

Figure 18. General layout of the FEBEX test. The bentonite instrumented sections are indicated

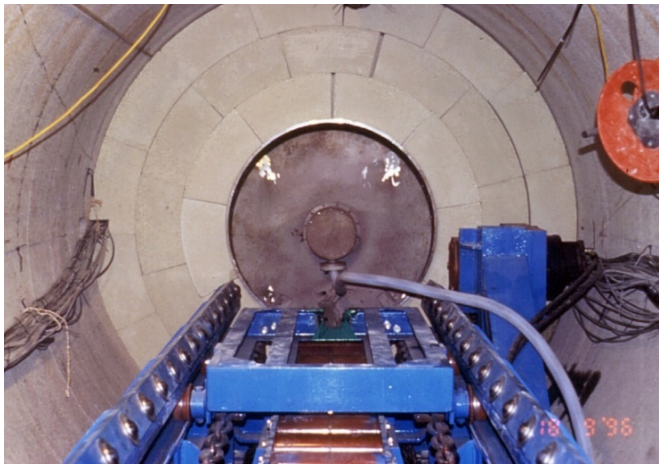

Figure 19. Cross-section of the FEBEX test showing the heater surrounded by compacted bentonite blocks

The FEBEX test lasted nearly 20 years from the start of tunnel excavation until the completion of the final dismantling. The dates of the most relevant events in the experiment are listed in Table 5. The heating stage of the experiment started on the 27th February 1997. This is taken as date zero to define a common time scale. The sequence of the initial heating stage was as follows:

- During an initial period of 20 days, a constant power of 1200 W per heater was applied, with the aim of identifying the thermal response of the system and adjusting the control algorithms.
- Over the next 33 days, the power was increased to 2000 W per heater and maintained constant in order to reach the desired maximum temperature of 100 °C on the bentonite/liner contact surface.
- Finally, on 21st April 1997 (day 53), the system was changed to temperature control maintaining a maximum temperature of 100°C on the liner/bentonite contact surface. Heater power was automatically adjusted to keep this condition throughout the experiment.

Table 5. Dates of the most relevant events in the FEBEX test

Date	Event
25/09/1995	Start of tunnel excavation
30/10/1995	End of tunnel excavation
01/07/1996	Start of test installation
15/10/1996	End of test installation
27/02/1997	Heaters switched on (date zero)
28/02/2002	Heater #1 switched off
19/07/2002	End of first dismantling
20/04/2015	Heater #2 switched off
20/07/2015	End of final dismantling

After 5 years of heating, the test was partially dismantled. Heater #1 was extracted and most of the bentonite surrounding it was removed (Figure 20). The remaining experiment was sealed with a shotcrete plug. After 18.4 years of heating, Heater #2 was switched off and the final dismantling took place. The criterion of keeping the maximum temperature at 100ºC was maintained unchanged in Heater #2 throughout the experiment, including the period of the first dismantling operations. At each dismantling, a great number of samples were extracted to determine their dry density and water content. The determinations were made on site immediately after extraction.

For comparison purposes, the modelling teams were requested to provide evolutions and distributions of temperatures and relative humidity as well as evolutions of total stresses at selected points and sections.

Radial distributions of dry density, water content and degree of saturation at a number of sections were also required for the two dismantling operations.

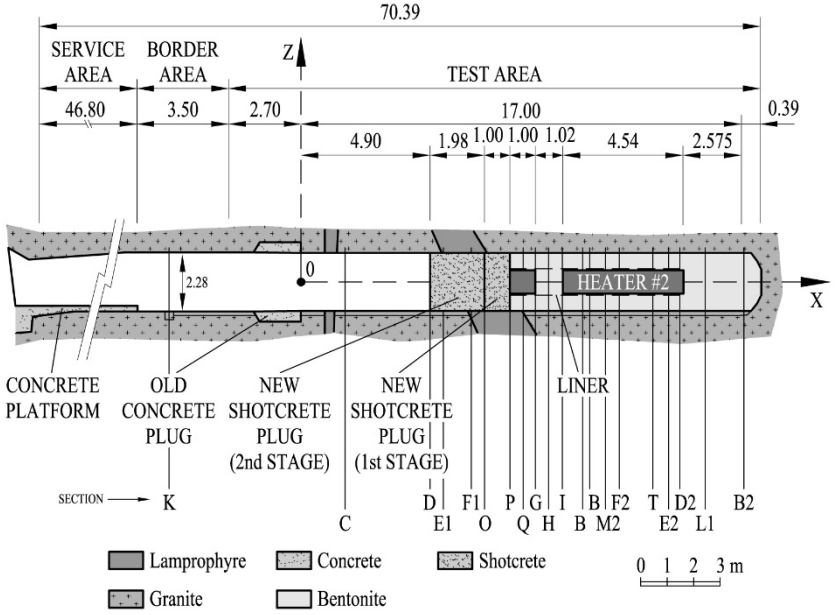

Figure 20. Configuration of the FEBEX test after completing the first dismantling

7. FEBEX test: modelling features

The main features of the formulations used in the analyses of the FEBEX test are listed in Table 6. They are natural extensions of the HM formulation incorporating thermal effects by adding the equations of energy conservation and heat transport. IGN[14] and KAERI use a fully coupled THM formulation (i.e. coupled in all directions) whereas JAEA and NCU consider the effect of the TH problem on the mechanical one but not vice versa. For this analysis, JAEA employs a new code, DACSAR, to solve the mechanical problem in the bentonite barrier.

Table 6. Main features of the FEBEX analyses

Team	Coupling	Computer code	Geometry	Variable intrinsic permeability	Vapour transport	Mechanical constitutive model
IGN	THM (fully coupled)	COMSOL 2D	2D (axisym.)	Yes	Yes	Non-linear elastic + swelling term
JAEA	TH (rock) TH>M (bent.)	THAMES 3D (TH) DACSAR 2D (M)	3D (TH) 2D (M)	No	Yes	Unsaturated elasto-plastic model
KAERI	THM (fully coupled)	TOUGH2-MP (H) + FLAC 3D (M)	3D wedge (axisym.)	Yes	Yes	Elasto plastic model (BBM)
NCU	TH > M	HYDROGEOCHEM 5.3	3D	No	No	Linear elastic + swelling term

The dominant mechanism for heat transport is conduction governed by Fourier's law. Although heat advection is generally contemplated in the formulations, it has a negligible effect in this particular problem. The dependence of thermal conductivity on degree of saturation is considered by all teams. Vapour generation and transport, potentially important in non-isothermal situations, is included by all teams except NCU. Diffusion controlled by vapour density gradients (noting that vapour density is strongly influenced by temperature and water suction) is the main mechanism underlying vapour flow. The influence of temperature on hydraulic conductivity via the thermally-induced variation of viscosity is taken into account by IGN and KAERI. As in the EB analyses, JAEA and NCU neglect the variation of permeability with dry density. Temperature-dependent retention curves are only used by IGN.

The mechanical constitutive models adopted are similar to those used in the EB analyses apart from JAEA that uses an unsaturated elasto plastic model in which the hardening parameter depends on degree of saturation[18]. Thermomechanical effects are introduced via a linear expansion coefficient by all teams except JAEA. In addition, KAERI uses a non-isothermal version of the BBM model that introduces a variation for yield surface with temperature. IGN incorporates thermal effects on the mechanical behaviour by indirect means, through the variation of the mass water content coefficient and by thermally-induced changes in dry density.

The modelling teams simulated the entire history of the test: excavation and ventilation of the tunnels, installation of the experiment, power-controlled heating stage, temperature-controlled heating, first dismantling, subsequent temperature-controlled heating and final dismantling. NCU uses a 3D domain for the THM calculations and JAEA for the TH analysis. The rest of the simulations are performed assuming axisymmetric conditions (KAERI uses a 3D mesh but with geometric symmetries that make it equivalent to axisymmetry).

The initial conditions in the bentonite barrier for the various analyses are shown in Table 7. They are all very similar; the only differences arise in the initial value of relative humidity (or suction), consequence of the use of different retention curves. It can be noted that all teams adopt the average value of dry density for the bentonite, no specific modelling of the initial gaps in the barrier has been undertaken.

Table 7. Initial conditions in the bentonite barrier

Team	Initial dry density (g/cm^3)	Initial porosity	Initial mass water content (%)	Initial degree of saturation (%)	Initial suction (MPa)	Initial relative humidity (%)
IGN	1.60	0.41	14.1	56	135	36
JAEA	1.60	0.41	14.4	57	106	43.3
KAERI	1.60	0.41	14.0	55	129.8	37.7
NCU	1.62	0.4	13.4	54.2	120	40

As in the EB test, parameters were selected based on information provided in the Task specifications, technical literature and previous experience. The main thermal parameters are presented on Table 8; quite similar values are adopted by all teams. The main hydraulic, mechanical and hydromechanical parameters are collected in Table 9. It can be noted that the value of permeability used by JAEA is about an order of magnitude higher compared to the other teams; it corresponds to a dry density of 1.5 g/cm^3. This value is maintained constant throughout the analysis and the effects of temperature, porosity and temperature are ignored. The main differences between the teams concern the values of swelling pressure, reflecting the variety of mechanical constitutive models.

Table 8. Main thermal parameters for bentonite and rock

Team	Bentonite initial thermal conduct. (W/mK)	Bentonite initial sat. thermal conduct. (W/mK)	Bentonite initial dry thermal conduct. (W/mK)	Bentonite solid specific heat (J/kg K)	Rock thermal conduct. (W/mK)	Rock specific heat (J/kg K)
IGN	0.77	1.28	0.57	749	3.6	920
JAEA	0.79	1.26	0.57	749.1	3.6	800
KAERI	0.76	1.28	0.57	749.1	3.6	920
NCU	0.88	1.30	0.4	830	3.3	920

Table 9. Main hydraulic, mechanical and thermomechanical parameters for bentonite and rock

Team	Initial intrinsic permeability (m^2)	Initial intrinsic saturated permeability (m^2)	Rock intrinsic saturated permeability (m^2)	Initial swelling pressure* (MPa)	Linear thermal expansion coefficient (K^{-1})
IGN	1.71×10^{-22}	1.65×10^{-21}	5.0×10^{-18}	5.82	10^{-5}
JAEA	1.48×10^{-21}	8.0×10^{-21}	5.0×10^{-18} (+)	6.56	Not included
KAERI	2.50×10^{-22}	1.5×10^{-21}	5.0×10^{-18}	4.78	$1.5\ 10^{-4}$
NCU	3.10×10^{-22}	2.0×10^{-21}	5.0×10^{-18}	2.71	10^{-5}

* Swelling pressure under 1-D oedometric conditions

(+) Rock permeability: 5.0×10^{-18} m^2 vertical direction, 5.0×10^{-19} m^2 horizontal direction

8. FEBEX test: modelling results

This section contains the comparisons between the results obtained in the analyses and the measurements. The codes and labels of the modelling teams are the same as for the EB test (Table 4). Only some selected results, representative of the analyses performed, are shown. As indicated above, after a short power-controlled stage of the test, the experiment was run under temperature control; the power of the heaters was adjusted so that the maximum temperature in the bentonite (in contact with the liner) was 100ºC. The analysis by IGN simulated the actual control of the test, adjusting the power so that the temperature at the liner/bentonite contact point corresponding to the centre of the heater remained constant and equal to 100ºC. The other teams applied a constant 100ºC (97ºC in the case of NCU) as a boundary condition to the entire contact between liner and barrier.

The evolutions of computed and measured heater power are shown in Figures 21 (Heater #1) and 22 (Heater #2). It can be observed that the power of Heater #2 is about 10% higher than that of Heater #1. The reasons for this observed difference have not been identified. In contrast, all the analyses obtain practically the same power for the two heaters. Most modelling teams obtained quite good values for the power of Heater #1 whereas the power of Heater #2 is somewhat underestimated because of the difference indicated above. The four modelling teams use very similar thermal parameters and, therefore, they obtain similar results although JAEA appears to underestimate somewhat the heater power in the period before first dismantling.

Two typical examples of observed and calculated temperatures are presented in Figures 23 and 24. Temperatures are mostly well reproduced by the modelling teams. This is helped by the fact that the experiment is temperature-controlled, but it is still necessary to track adequately the changes in thermal conductivities with degree of saturation. Although all teams use similar thermal conductivity parameters, NCU analyses tend to fall in the upper range of results (despite applying a 97º C temperature boundary condition) whereas JAEA results tend to lie on the lower range. The adoption by IGN of a more realistic condition for heater power control does not appear to lead to significantly different results in terms of temperatures and/or heater power.

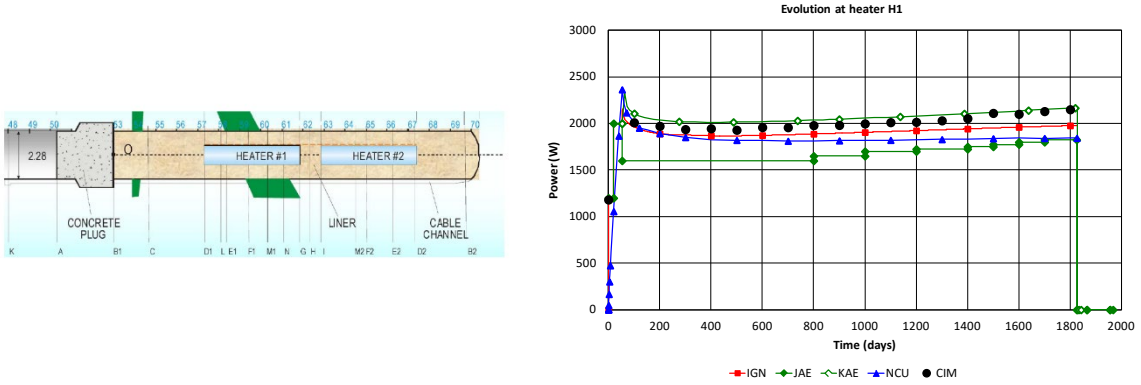

Figure 21. Modelling results vs. observations. Evolution of heater power. Heater #1.

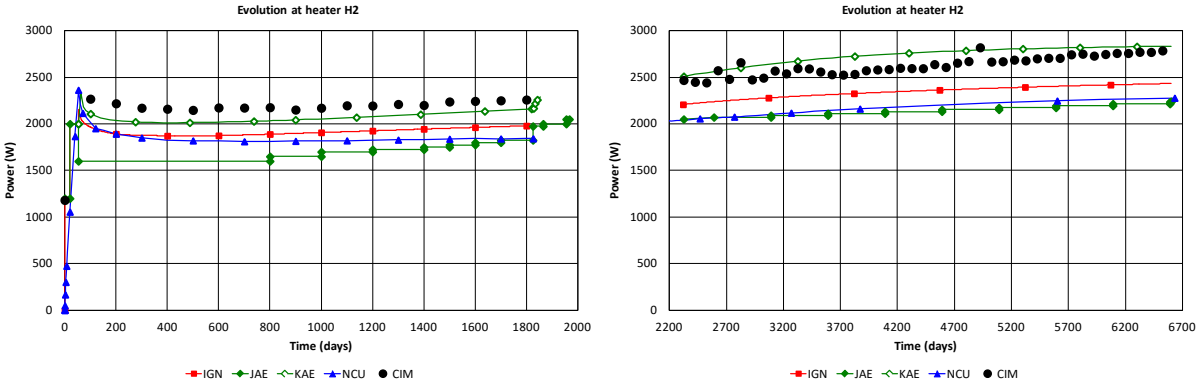

a) b)

Figure 22. Modelling results vs. observations. Evolution of heater power. Heater #2. a) before first dismantling, b) between first and second dismantling

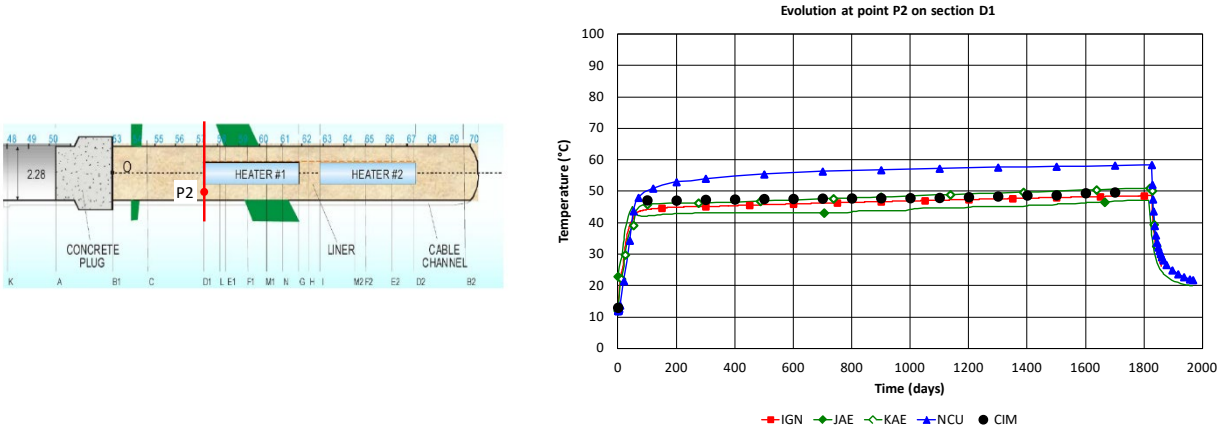

Figure 23. Modelling results vs. observations. Evolution of temperature at intermediate point P2. Section D1

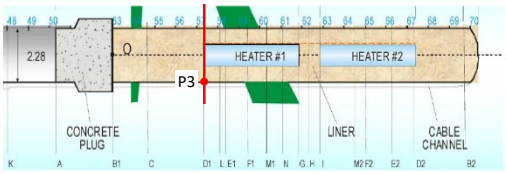

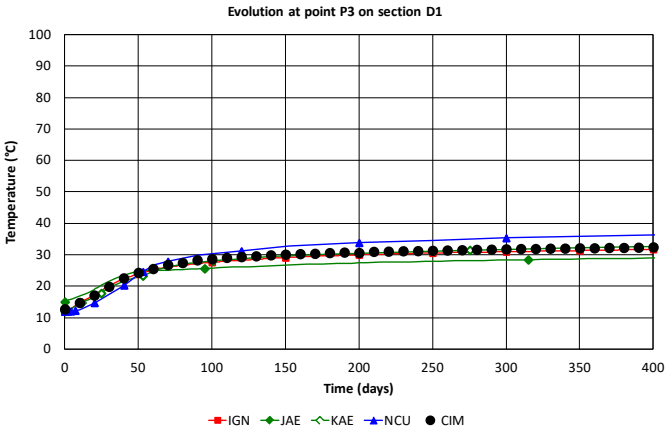

Figure 24. Modelling results vs. observations. Evolution of temperature at point P3 near the rock. Section D1

All analyses simulate adequately the progressive hydration of the barrier located around the heaters reflected in the examples of evolutions of relative humidity shown in Figures 25 and 26. Focusing on the behaviour close to the heaters (Figure 25), all the analyses (except NCU's) simulate the initial drying of the bentonite and a transient peak of relative humidity due to the passing of a vapour front. NCU does not reproduce those features because vapour transfer is not included in their current formulation.

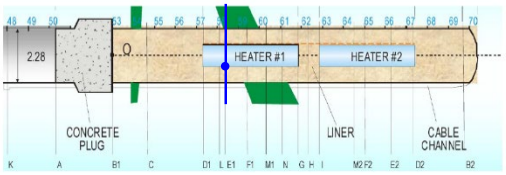

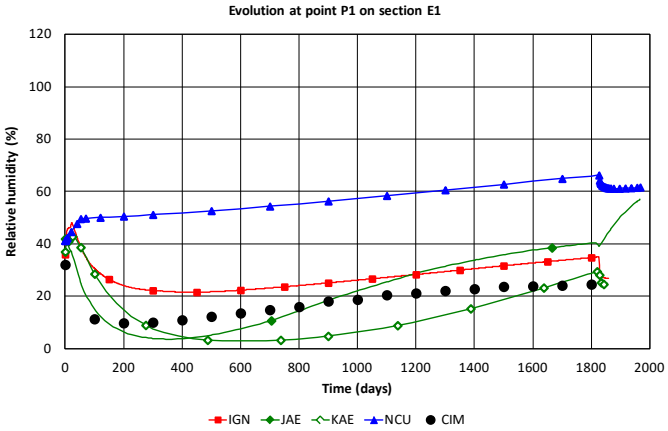

Figure 25. Modelling results vs. observations. Evolution of relative humidity at point P1 close to the heater. Section E1

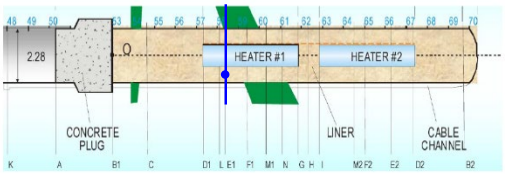

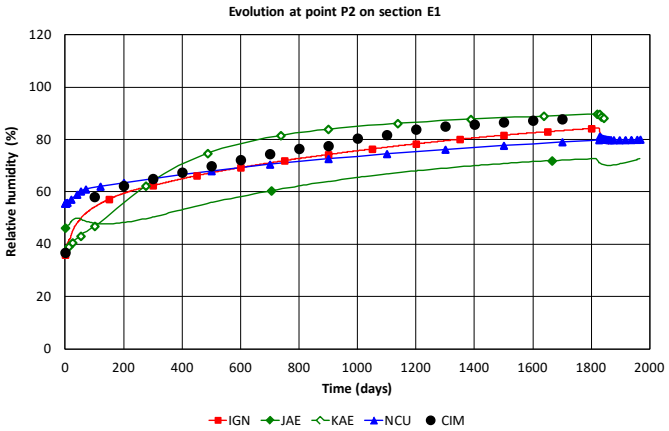

Figure 26. Modelling results vs. observations. Evolution of relative humidity at intermediate point P2 close to the heater. Section E1

The measurement of total stresses is commonly subject to a significant degree of uncertainty, so no exact reproduction of the observed evolution of total stresses is expected (e.g. Figure 27). Generally, the modelling teams report an increasing value of total stress associated with the progress of hydration; most computed magnitudes of total stresses at the time of first dismantling are generally quite realistic. NCU obtains low values of total stresses due to the small swelling pressure that results from the constitutive model and parameters adopted (Table 9). The absence of thermal expansion of the bentonite in JAEA analysis may also contribute to a smaller prediction of radial stresses.

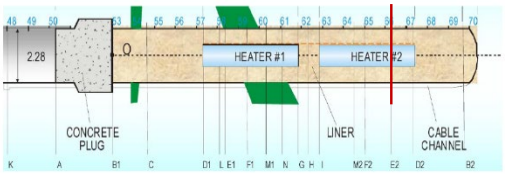

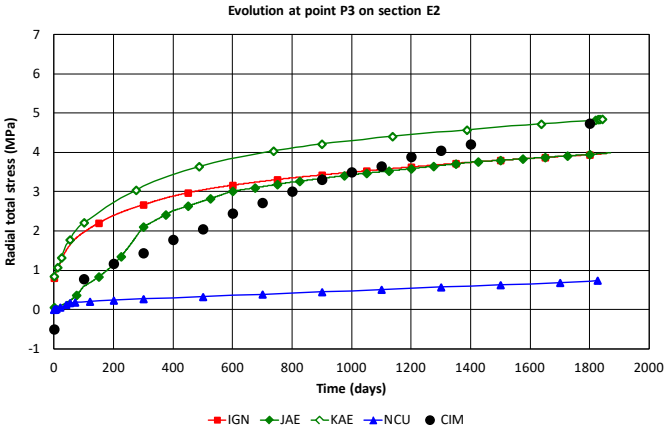

Figure 27. Modelling results vs. observations. Evolution of radial total stress at point P3 close to the rock. Section E2

Figure 28 presents characteristic results of the first dismantling for a section located in the zone affected by the thermal effects of the heater. It can be noted that the degree of saturation is around 100% near the

rock but it is much lower close to the heater where drying has initially taken place. In fact, after 5 years of heating and natural hydration, the bentonite close to the heater has just recovered the initial degree of saturation. This pattern of variation is captured by all the models although the drying reported by JAEA and NCU is less than observed. The values well above 100% in the zone adjacent of the rock reported by IGN do not quite correspond to the measurements at this stage. The final state of the barrier around the heaters, in terms of dry density, is non-homogeneous, with lower dry density near the rock and a higher dry density near the heater. Since both the rock and the heater/liner system are stiff, the average dry density is bound to remain approximately constant throughout. All analyses (except NCU's) result in an adequate reproduction of the type of dry density distribution observed with a range of values somewhat narrower than observed. NCU analysis yields a constant value across the barrier because of the limitations of their current formulation.

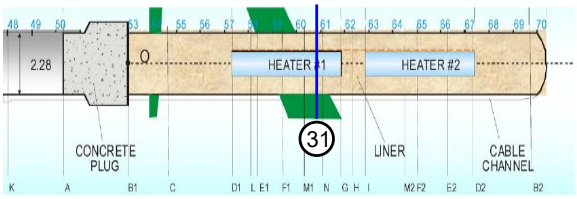

a)

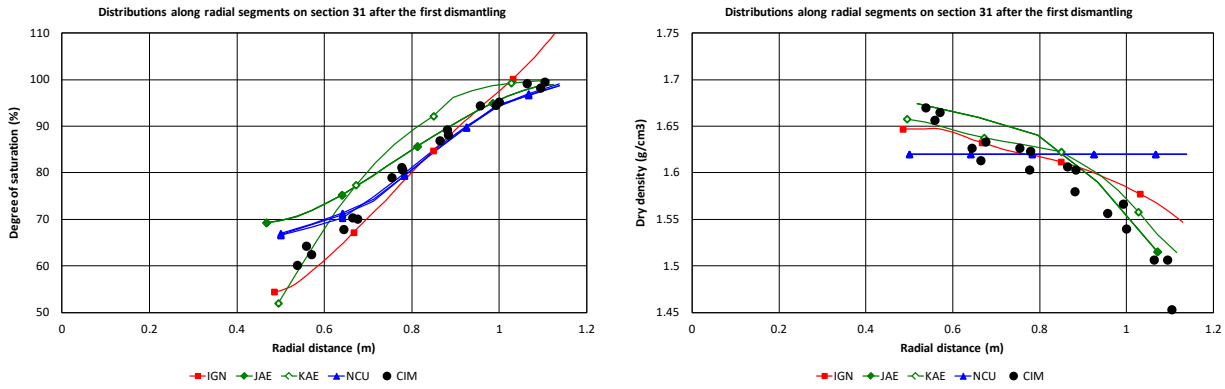

b) c)

Figure 28. Modelling results vs. observations in the first dismantling. a) Sampling section 31, b) distributions of degree of saturation, c) distributions of dry density

Computed and observed radial distributions of degree of saturation and dry density obtained in the final dismantling from the samples extracted in Section 43 are plotted in Figure 29. It can be observed that the barrier has become saturated with degrees of saturation just above 100%, a characteristic result in highly

compacted saturated FEBEX bentonite. KAERI and NCU predict a barrier very close to saturation in the heater zone. In contrast, JAEA predicts a quite unsaturated state across most of the barrier. IGN obtains an intermediate result.

In contrast, the dry density has not become homogenous upon reaching saturation; the barrier exhibits a non-homogenous state, a lower dry density close to the rock and a higher dry density close to the heater, even when the barrier has become saturated. All the analyses, except NCU, yield similar distributions of dry density. As indicated above, NCU reports a constant dry density, as the current formulation does not incorporate variations of porosity due to suction and/or stress changes

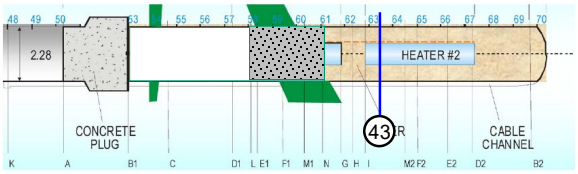

a)

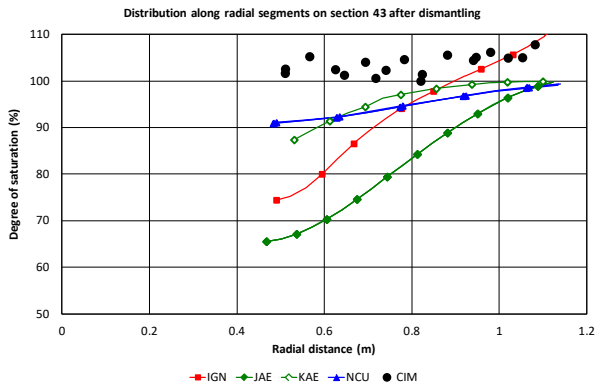

b)

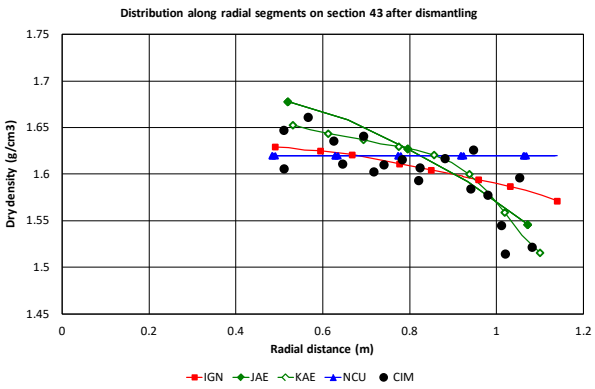

c)

Figure 29. Modelling results vs. observations in the final dismantling. a) Sampling section 43, b) distributions of degree of saturation, c) distributions of dry density

9. FEBEX test: discussion

All the teams have considered the bentonite barrier as a continuous material, joints and gaps present at the installation of the test have not been considered in the analyses. All teams have assumed as initial value the average dry density of the barrier and not the dry density of the blocks themselves.

Regarding the thermal aspects of the case, the observed heater power is well captured by the analyses, especially for Heater #1. The gentle increase of heater power with time is also well captured; this increase is a consequence of the thermo-hydraulic coupling associated with the variation of thermal conductivity with degree of saturation. Temperatures are also generally well reproduced by all the modelling teams. This result is not unexpected as the FEBEX test is temperature-controlled, but it still requires an adequate representation of the variation of thermal conductivity with degree of saturation, a feature incorporated in all formulations used.

All analyses reproduce the progressive hydration of the engineered barrier. The initial drying close to the heaters is obtained by all modelling teams that incorporate vapour transport in their formulations. The comparisons between computed and observed total stresses are hampered by uncertainties concerning the measurements, especially during the initial part of the test. In any case, the final computed stresses lie basically on the right range of magnitude.

An interesting observation can be extracted by comparing the distributions of degree of saturation and dry density in the first and second dismantling (Figure 30). Naturally, no comparison is possible in the same section, but section 31 (first dismantling) and section 43 (final dismantling) are located in the same position relative to Heaters #1 and #2, respectively. Therefore, it is reasonable to compare the two sections to examine the evolution of the state of the barrier between the first dismantling (5 years of heating) and the final dismantling (18.4 years of heating). As Figure 30, shows hydration has continued during this period until the barrier has become fully saturated. Interestingly, the distribution of dry density has remained unchanged. It appears that the heterogenous distribution of dry density generated in the early stages of the test remains fixed subsequently; there is no evidence of any tendency for the barrier to evolve towards a homogenous state.

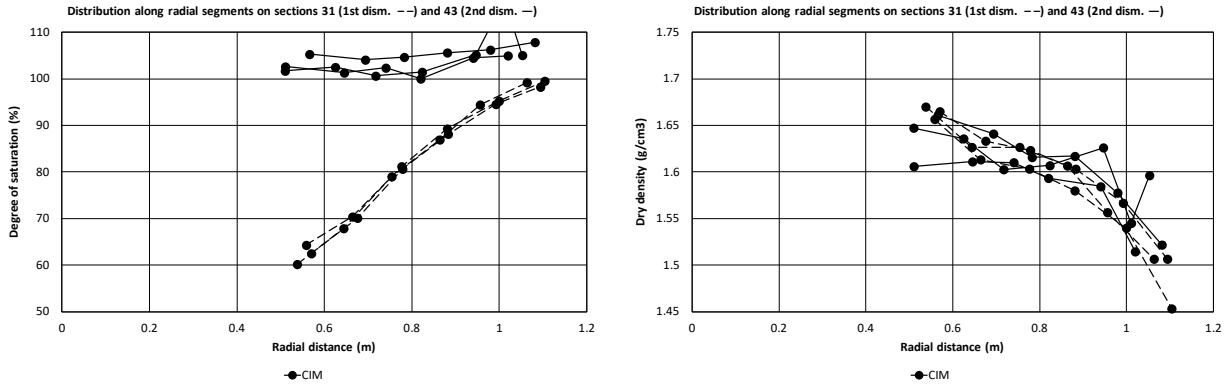

a) b)

Figure 30. a) Observed radial distributions at first dismantling (Section 31, dashed lines) and final dismantling (section 43, continuous lines). a) Degree of saturation, b) Dry density

It can be noted (Figure 29) that KAERI and NCU models yield final states of the barrier close to saturation, thus reproducing quite well the hydraulic evolution of the barrier although the computed final degrees of saturation are, in both cases, slightly lower than the observed ones. The analysis of IGN also shows an increase of degree of saturation, but of a lesser magnitude, so that the final state of the barrier is significantly less saturated than observed in the experiment. The reason for this difference does not appear to be related to the hydraulic conductivity that is similar in all three cases; a possible explanation may be linked to differences in retention curves, but this conjecture cannot be confirmed without further analyses. The degree of saturation computed by JAEA in the zone of the heater does not show any increase between the first and final dismantling so an unsaturated barrier is predicted at the end of the experiment. This result may be due to the adoption of a constant hydraulic conductivity throughout the analysis.

KAERI successfully computes no variation in the non-homogenous dry density distributions between the first and final dismantling in spite of having reached a nearly saturated state. Obviously, the formulation and the mechanical constitutive model used are capable of reproducing the general evolution of the barrier as observed in the test. IGN also computes practically unchanging non-homogenous distributions of dry density in spite of some significant degree of saturation increase. Some uncertainty remains, though, about what would be the state of the barrier on reaching full saturation taking into account that an elastic (albeit nonlinear) mechanical constitutive model is used in the calculations. JAEA also reports unvarying

distributions of dry density but, in this case, the significance of this result is limited because there are practically no changes in mass water content and degree of saturation between the two dismantling events.

10. Overview and concluding remarks

Four modelling teams have simulated the EB and FEBEX experiments and have provided results for comparison with test observations. A range of computer codes have been employed: COMSOL (IGN), THAMES (JAEA) TOUGH2-MP/FLAC 3D (KAERI) and HYDROGEOCHEM 4.3/5.3 (NCU). In addition, the DACSAR 2D code has been used by JAEA to solve the mechanical problem in the simulation of the FEBEX test. Normally, 2D geometries have been used to represent the domains of analysis, plane strain in case of the EB test and axisymmetric in the case of the FEBEX test. 3D geometries have been used by IGN in the EB modelling and by JAEA (only TH) and NCU in the FEBEX modelling. No apparent advantages have been obtained from the use of the more demanding, in terms of computing resources, 3D configurations.

All the analyses performed have been based on coupled TH and THM formulations. They involve the solution of the equations of water mass balance and liquid flow, equilibrium and, for non-isothermal problems, energy balance and heat transport. KAERI also incorporated and solved the air balance and gas flow equations. The thermal formulation is centred on heat conduction governed by Fourier's law. The dependence of thermal conductivity on degree of saturation is contemplated by all the formulations. As the consideration of vapour transport is important in non-isothermal problems, the phenomenon is incorporated in all the formulations except by NCU.

The hydraulic formulation is quite similar in all cases. Water flow is governed by Darcy's law with hydraulic conductivity dependent on degree of saturation via a relative permeability relationship, generally represented by a power law. IGN and KAERI also incorporate the variation of intrinsic permeability with dry density, an important feature to account for the effect of local porosity variations during the test. Temperature-dependent liquid viscosity is considered by IGN and KAERI introducing, in this way, a thermal effect on hydraulic conductivity. Retention curves are generally defined by expressions based on

the van Genuchten equation; only IGN incorporates effects of temperature and dry density in retention curves. The main departure from the standard conventional hydraulic formulation has been introduced by IGN by considering simultaneously the presence of the water in the pores and in the interlayer space. Consequently, degrees of saturation higher than 100% can be computed if they are referred to the pore volume.

There is a wider variety of mechanical constitutive models adopted in the analyses. IGN and NCU use an elastic model plus a swelling term (dependent on degree of saturation) whereas KAERI employs an elasto-plastic model (BBM) that incorporates suction effects. JAEA adopts an elastic model plus a swelling term for the EB modelling and an unsaturated elasto-plastic model for the FEBEX simulation. Net stresses are used by all teams in the unsaturated range. Thermal effects on the mechanical constitutive laws are introduced in different ways by IGN and KAERI. All teams except JAEA incorporate the thermomechanical coupling associated with a constant thermal expansion coefficient.

Considering the complete TH and THM formulations, it is noteworthy that there are no basic differences in the models used for pellets and blocks in spite of the obvious dissimilarities in texture and pore size distribution, at least in their initial state. The same formulation is used for both material types, the only distinction being their different initial porosities.

Regarding the overall performance of the numerical analyses carried out, the general conclusion is that they are able to represent adequately the global TH and THM behaviour of the experiments modelled. The most important phenomena and their couplings appear to be incorporated in an appropriate manner. Additional features such as the incorporation of the gas flow equation (KAERI) or the consideration of interlayer water does not appear to affect the results of the analyses significantly. There are however a number of shortcomings in some formulations that affect the ability to capture some important aspects of the tests. For instance, the fact that the permeability does not depend on dry density in the JAEA formulation impacts the calculations of the progress of hydration. In the case of the NCU formulation, the lack of vapour transport affects the predictions of the bentonite hydraulic behaviour, especially close to the heater, and the

invariance of dry density with respect to suction and stresses prevents the simulation of barrier heterogeneity and its evolution.

As noted above, the Task does not involve any blind predictions; the experimental results were available to the modelling teams from the start. Therefore, the results presented cannot provide conclusive information on the predictive capabilities of the modelling. In fact, those predictive capabilities may not be high given the sensitivity of some processes to various parameters; the progress of hydration and barrier saturation time being prime examples.

It is also important to realize that an adequate reproduction of one-off large-scale in situ tests does not necessarily imply that all individual phenomena and processes are well represented in the modelling. To identify the effects of individual processes, it is necessary to perform well-designed and closely controlled tests specifically devised to elucidate individual aspects of behaviour. It is probably necesaary that such tests have to be performed at a smaller scale, in a laboratory environment.

To conclude, a paradox involving the two experiments analysed in this Task can be noted. In the EB experiment, the bentonite barrier starts in a very heterogeneous vertical configuration (blocks and pellets) and yet it attains practically full homogenization in that direction. In the FEBEX experiment, the initial configuration is basically homogenous, hydration and heating are axisymmetric, but the final stage of the barrier is unmistakably heterogeneous. It suggests that a full understanding of the behaviour of bentonite barriers remains challenging and may require further work..

Acknowledgements

DECOVALEX is an international research project comprising participants from industry, government and academia, focusing on development of understanding, models and codes in complex coupled problems in sub-surface geological and engineering applications; DECOVALEX-2019 is the current phase of the project. The authors appreciate and thank the DECOVALEX-2019 Funding Organisations: ANDRA, BGR/UFZ, CNSC, US DOE, ENSI, JAEA, IRSN, KAERI, NWMO, RWM, SÚRAO, SSM and Taipower for their financial and technical support of the work described in this report. The statements made in the

report are, however, solely those of the authors and do not necessarily reflect those of the Funding Organisations.

Martin Hasal (IGN) contribution was supported by the European Regional Development Fund under the project AI&Reasoning (reg. no. CZ.02.1.01/0.0/0.0/15 003/0000466)

The JAEA contribution was partly funded by the Ministry of Economy, Trade and Industry of Japan (METI) through the program "The project for validating near-field system assessment methodology in geological disposal" (JFY2018).

The KAERI contribution was supported by the Nuclear Research and Development Program of National Research Foundation of Korea (NRF) and funded by the Minister of Science, ICT, and Future Planning (NRF-2017M2A8A5014857).

References

1. Gens A. Soil-environment interactions in geotechnical engineering. The 47 Rankine Lecture. *Géotechnique*, 2010; 60:3-74.

2. Gens A, Alcoverro J, Blaheta R, Hasal M, Michalec Z, Takayama Y, Lee C, Lee J, Kim GY, Kuo C-W, Kuo W-J, Lin C-Y. *DECOVALEX-2019. Task D: INBEB. Final Report*. LBNL-2001267. Lawrence National Berkeley Laboratory; 2019.

3. Thury M., Bossart, P. The Mont Terri rock laboratory, a new international research project in a Mesozoic shale formation, in Switzerland. *Engineering Geology*, 1999; 52: 347–359.

4. Mayor JC, García-Siñériz JL, Alonso E, Alheid H-J, Blümling P. Engineered barrier emplacement experiment in Opalinus Clay for the disposal of radioactive waste in underground repositories. In: Bossart P and Nussbaum C, eds. *Mont Terri Project - Heater Experiment, Engineered Barriers Emplacement and Ventilation Tests*. Rep. Swiss Geol. Survey No. 1; 2007: 115-179.

5. Villar MV. *Thermo-hydro-mechanical characterization of a bentonite from Cabo de Gata. A study applied to the use of bentonite sealing material in high level radioactive waste repositories. [Ph.D. Thesis].* ENRESA Technical Publication 01/2002, Madrid. 2002.

6. Villar MV, Lloret A. Variation of the intrinsic permeability of expansive clays upon saturation: measurement with gas and water. In: K. Adachi, M. Fukue, eds. *Clay science for engineering*. Balkema; 2001: 259‑266.

7. ENRESA. *FEBEX project. Full-scale engineered barriers experiment for a deep geological repository for high level radioactive waste in crystalline host rock. Final report.* Publicación Técnica 1/2000, ENRESA, Madrid. 2000.

8. Pintado X, Ledesma A, Lloret A. Backanalysis of thermohydraulic bentonite properties from laboratory tests. *Engineering Geology*. 2002; 64: 91‑115.

9. Lloret A, Villar MV, Sánchez M, Gens A, Pintado X, Alonso EE. Mechanical behavior of heavily compacted bentonite under high suction changes. *Géotechnique*. 2003; 53(1): 27‑40.

10. Alonso EE, Hoffmann C. Modelling the field behaviour of a granular expansive barrier. *Physics and Chemistry of the Earth.* 2007; 32: 850-865. doi: 10.1016/j.pce.2006.04.039.

11. Hoffmann C, Alonso EE, Romero E. Hydro-mechanical behaviour of bentonite pellet mixtures. *Physics and Chemistry of the Earth.* 2007; 32: 832-849. doi: 10.1016/j.pce.2006.04.037

12. Mayor, J.C. and Velasco, M. (2014) *Long-term Performance of Engineered Barrier Systems PEBS. EB dismantling Synthesis report (DELIVERABLE-Nº: D2.1-8).* Seventh Euratom Framework Programme for Nuclear Research &Training Activities (2007-2011) Contract number: FP7 249681. 2014.

13. van Genuchten R. Calculating the unsaturated hydraulic permeability conductivity with a new closed-form analytical model. *Water Resour. Res*. 1978; 37(11): 21–28.

14. Michalec Z., Blaheta R., Hasal M., Ligursky T. Fully coupled thermo-hydro-mechanical model with oversaturation and its validation to experimental data from FEBEX experiment, submitted to *International Journal of Rock Mechanics and Mining Sciences*, 2020 (this issue).

15. Jacinto AC, Villar MV, Ledesma A. Influence of water density on the water-retention curve of expansive clays. *Geéotechnique.* 2012; 62(8): 657–667. http://dx.doi.org/10.1680/geot.7.00127

16. Alonso EE, Gens A, Josa A. A constitutive model for partially saturated soils. *Géotechnique*. 1990; 40(3): 405–430.

17. Keusen HR, Ganguin J, Schuler P, Buletti M. *Grimsel Test Site. Geology*. Technical Report NTB 87-14E. Baden: Nagra. 1989.

18. Ohno S, Kawai K, Tachibana S. Elasto-plastic constitutive model for unsaturated soil applied effective degree of saturation as a parameter expressing stiffness. *Journal of the Japan Society of Civil Engineers JSCE*. 2007; 63 (4): 1132-1141 (in Japanese).